IOPscience iopscience.iop.org

Home Search Collections Journals About Contact us My IOPscience

Particle clustering in turbulent premixed flames

This article has been downloaded from IOPscience. Please scroll down to see the full text article.

2011 J. Phys.: Conf. Ser. 333 012002

(http://iopscience.iop.org/1742-6596/333/1/012002)

View the table of contents for this issue, or go to the journal homepage for more

Download details:
IP Address: 83.185.44.192
The article was downloaded on 25/01/2012 at 17:26

Please note that terms and conditions apply.

Journal of Physics: Conference Series **333** (2011) 012002 doi:10.1088/1742-6596/333/1/012002

Particle clustering in turbulent premixed flames

Battista F.[1], **Picano F.**[1], **Troiani G.**[2], **& Casciola C.M.**[1]

[1] Dipartimento di Ingegneria Meccanica e Aerospaziale, "La Sapienza" University of Rome, Italy
[2] C.R. ENEA Casaccia, Rome, Italy

E-mail: francesco.picano@uniroma1.it

Abstract. Transport of inertial particles in turbulent reacting flows is frequent in a number of engineering and natural systems. Aim of this work is to illustrate the effect of the fluctuating instantaneous flame front on the particle spatial distribution. To this purpose a Direct Numerical Simulation of a Bunsen premixed flame seeded with small inertial particles is performed. The flamelet Stokes number St_{fl}, defined as the ratio between the particle relaxation time and the flame front time scale, is found to be the proper parameter to characterize the particle dynamics in a premixed flame. Clustering of inertial particles is apparent, especially beyond the flame front. The amount of particle segregation is here quantified by the clustering index and two distinct contributions are found to interplay. The first is independent of the particle inertia and affects also tracers. Actually it is associated to the abrupt variation of the particle concentration induced by the fluid expansion across the flame front. The second effect is mainly due to the time lag associated to the particle inertia that, in proximity of the front, affects both the mean and the fluctuation of the particle number in a fixed volume. The global effect results in an intense clustering of the inertial particles in the flame brush region with a maximum for particles with flamelet Stokes number: $St_{fl} = \mathcal{O}(1)$.

1. Introduction

Particles with different inertia and dimension dispersed in reacting flows are frequently found in many engineering or natural applications, e.g. solid fueled rocket engines or soot formation.

The inertial particle dynamics has been addressed in several incompressible flow configurations, e.g. homogeneous flows, pipe and channel flows, see e.g. [1, 2] for recent reviews. Peculiar transport phenomena have been discussed, such as small-scale clustering [3, 4, 5, 6, 7] which consists of a loss of homogeneity of the particle distribution that leads to the formation of void regions and particle clusters, turbophoresis in the wall bounded flows [8, 9, 10, 11] which amounts to a mean drift of the particles towards the wall and preferential accumulations in free jets [12, 13, 14, 15].

The inertial particle spatial distribution in presence of temperature fluctuations is addressed in [16]. The turbulent thermal diffusion in stably stratified flows induces a non uniform mean particle distribution which presents preferential segregation near the minimum of the mean temperature. The authors demonstrate that the *tangling* clustering occurring in presence of thermal fluctuations, via buoyancy effects, is more effective than the clustering observed in isothermal conditions.

In this framework, as far as the authors know, the interaction between inertial particle dynamics and the large temperature variations typical of reactive flows has not been investigated

Published under licence by IOP Publishing Ltd

in details. This issue is relevant for particle collisions and coalescence in reactive flows, e.g. in problems concerning soot growth.

In turbulent premixed combustion, new phenomenologies arises, e.g. interactions with thermal expansion and intense temperature gradients. As a matter of fact, the flame front induces sudden fluid accelerations that could be not accommodated by finite inertia particles.

Aim of the present work is to discuss the effects induced by the simultaneous presence of finite inertia and flame front fluctuations by addressing a DNS of premixed turbulent flame endowed with inertial particles. In order to isolate the effects of inertia from concurrent effects, thermophoresis and gravitational forces are neglected. The main effect we observe is the clustering of the particles in the region spanned by the instantaneous turbulent flame front, the so called flame brush region. Clustering is quantified in terms of clustering index, see e.g. [17]. Also particles with negligible inertia present the intermittent spatial distribution typical of clustering. This feature is explained by a simple model based on the Bray-Moss-Libby assumptions for flamelets [18]. Additional intermittency is found for particle with finite inertia which present an increased clustering especially in flame brush.

2. The model for inertial particle dynamics

The basic model to address inertial particle transport consist of a very diluted suspension of small spherical particles is here considered where inter-particle collisions and force feedback on the fluid are negligible. The particle mass density is assumed much larger than the fluid one, $\rho_p/\rho_f \gg 1$ so that the particle dynamic is forced by the only Stokes drag [19, 20],

$$\begin{cases} \dfrac{d\boldsymbol{x}_p}{dt} = \boldsymbol{v} \\ \dfrac{d\boldsymbol{v}}{dt} = \dfrac{\boldsymbol{u}(\boldsymbol{x},t)|_{\boldsymbol{x}=\boldsymbol{x}_p} - \boldsymbol{v}}{\tau_p} \end{cases} \tag{1}$$

where $\boldsymbol{x}_p$ and $\boldsymbol{v}$ are the particle position and velocity, respectively, while $\boldsymbol{u}(\boldsymbol{x},t)|_{\boldsymbol{x}=\boldsymbol{x}_p}$ is the fluid velocity at particle position. $\tau_p = d_p^2/(18\,\nu)(\rho_p/\rho_f)$ is the particle relaxation time quantifying the time lag of the particle in following fluid velocity fluctuations (here d_p is the particle diameter, ρ_p and ρ_f the particle and fluid density, respectively, and ν the fluid kinematic viscosity). We neglect gravity and the thermophoretic force which may affect the motion of small particles in reacting flows. Thermophoresis acts on very small particles (not considered in the present study) producing a drift towards the reactants. Actually, it is induced by unbalanced Brownian collisions across the steep temperature gradients of the flame front.

The proper parameter controlling particle dynamics is a suitably defined Stokes number, ratio of particle relaxation time to the relevant time scale of the flow. In turbulent premixed combustion the strong fluid acceleration due to the abrupt thermal expansion across the flame front provides the smallest fluid dynamics time scale, $\tau_{fl} = \delta_{fl}/\Delta u_{fl}$, where δ_{fl} is the thermal thickness of the laminar flame and Δu_{fl} the velocity jump across the front. The thermal thickness can be estimated as $\delta_{fl} = (T_b - T_u)/|\nabla T|_{sup}$, where T_b and T_u are the temperature of burned and unburned mixtures respectively, with $|\nabla T|_{sup}$ the norm of maximum temperature gradient. Across the flame front, thermal expansion drives a velocity jump $\Delta u_{fl} = S_{fl}\,(T_b/T_u - 1)$, with S_{fl} the laminar flame speed. In this framework the Stokes number controlling particle dynamics reads [21]

$$St_{fl} = \frac{\tau_p\, S_{fl}\,(T_b/T_u - 1)}{\delta_{fl}}\ . \tag{2}$$

We stress that the flamelet Stokes number defined above depends on the particle relaxation time τ_p and on the thermo-chemical properties of the flame, namely the temperature ratio T_b/T_u and

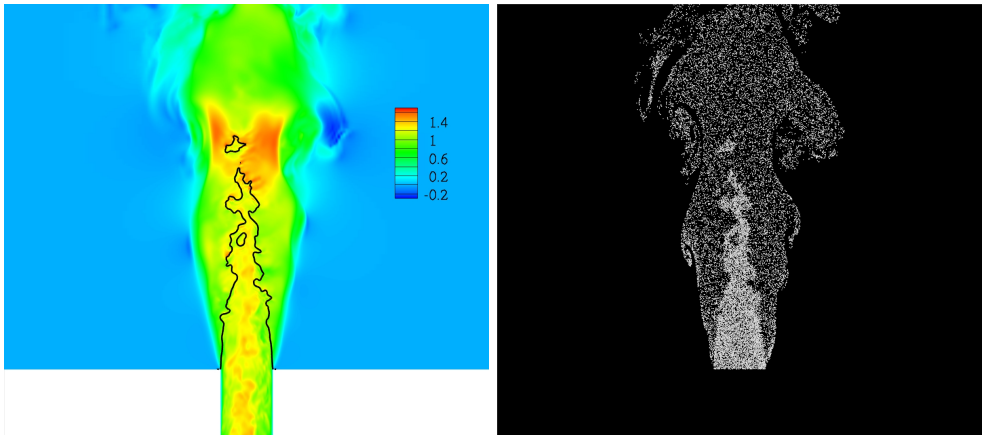

Figure 1. Right panel: instantaneous field of axial velocity fluid with contours and iso-level of reactants at $Y_R/Y_R^0 = 0.5$. Right panel: lighter particles $St_{fl} = 0.022$ instantaneous position.

the flamelet speed S_{fl} and thickness δ_{fl}. It should be remarked that usually τ_{fl} is smaller than the Kolmogorov time scale τ_η, e.g. here $\tau_\eta \simeq 2\,\tau_{fl}$.

3. Methodology

The problem is addressed by means of an Eulerian Direct Numerical Simulation (DNS) of a turbulent Bunsen burner coupled with a Lagrangian solver for particle evolution. The Eulerian algorithm discretizes the Low-Mach number formulation of the Navier-Stokes equations [22] in a cylindrical domain, which describes a low Mach number flow with arbitrary flame-induced density variations neglecting acoustics effects,

$$\frac{\partial \rho}{\partial t} + \boldsymbol{\nabla} \cdot (\rho \boldsymbol{u}) = 0 \tag{3}$$

$$\frac{\partial \rho \boldsymbol{u}}{\partial t} + \boldsymbol{\nabla} \cdot (\rho \boldsymbol{u}\boldsymbol{u}) = \frac{1}{Re} \boldsymbol{\nabla} \cdot \left[\mu \left(\boldsymbol{\nabla}\boldsymbol{u} + \boldsymbol{\nabla}\boldsymbol{u}^T\right)\right] - \boldsymbol{\nabla} p + \frac{1}{Fr^2} \rho \boldsymbol{f} \tag{4}$$

$$\frac{\partial \rho Y_R}{\partial t} + \boldsymbol{\nabla} \cdot (\rho Y_R \boldsymbol{u}) = \frac{1}{ReSc_R} \boldsymbol{\nabla} \cdot (\mu \boldsymbol{\nabla} Y_R) - \omega_R \tag{5}$$

$$\boldsymbol{\nabla} \cdot \boldsymbol{u} = \frac{1}{\mathcal{P}} \left[\frac{1}{RePr} \boldsymbol{\nabla} \cdot (\mu \boldsymbol{\nabla} T) + \frac{\gamma - 1}{\gamma} Ce\, \omega_R\right] \tag{6}$$

$$T = \frac{\mathcal{P}}{\rho} \tag{7}$$

with ρ, $\mathbf{u}$ and p the density, the velocity and the dynamic pressure, respectively- T, $\mathcal{P}$ Y_R and ω_R are the temperature, the thermodynamic pressure, the reactant concentration and its global reaction rate, respectively. μ is the dynamic viscosity of the mixture, $Re = \rho_0 U_0 L_0/\mu_0$ is the Reynolds number and $Pr = \mu_0/(\rho_0 \alpha)$ is the Prandtl number giving the ratio between thermal and viscosity of the mixture (here $Pr = 0.6$). The ratio between the heat capacity coefficient is denoted by γ (here $\gamma = 1.3$) and the ratio between mass and momentum transport reactant coefficient is given by the Smidth number $Sc_R = \mu_0/(\rho_0 D_\alpha)$ (here $Sc_R = 0.6$). The chemical kinetics is given by a simple one-step irreversible reaction transforming premixed fresh mixture R into combustion products P, with an Arrhenius model for the reaction rate: $\omega_R = Da\,(\rho Y_R) e^{T/T_a}$ (Da the nominal Damkohler number, T_a the activation temperature, Ce the non dimensional

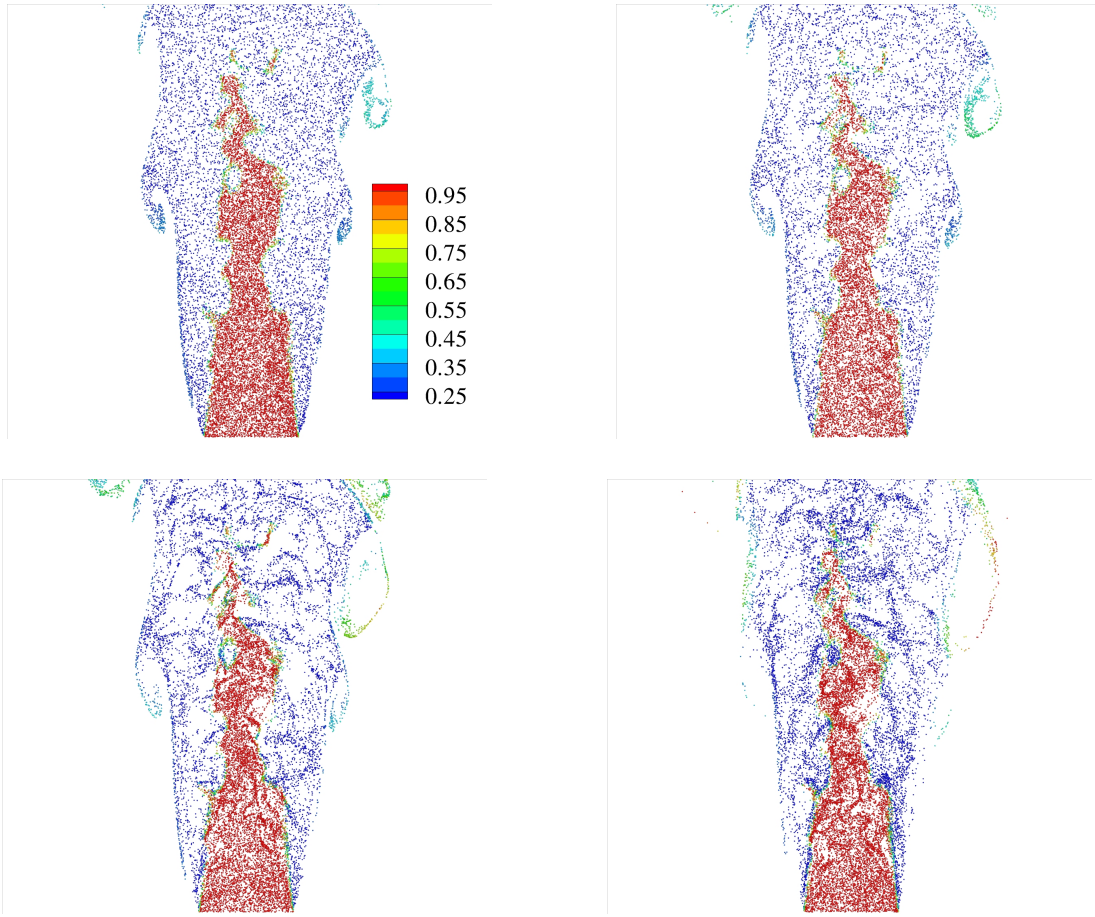

Figure 2. Thin slice of width $R/20$ in the axial-radial plane of the instantaneous particle configuration for different Stokes time. Top-left: $St_{fl} = 0.022$; Top-right: $St_{fl} = 0.54$; Bottom-left $St_{fl} = 2.16$; Bottom-right $St_{fl} = 8.65$. Colors denote the density of the fluid ρ/ρ_u at the particle position.

heat release). The model is tuned to reproduce a lean premixed methane-air Bunsen flame with equivalence ratio $\phi \sim 0.7$ ($T_b/T_u = 5.3$ imposed by the parameters $T_a/T_u = 30$, $Da = 45000$, $Ce = 18.5$), with temperature dependent viscosity according to Sutherland's law, $\mu \propto T^{1/2}$. The ratio of laminar flame speed to the bulk velocity at jet exit is $S_{fl}/U_0 \simeq 0.05$, with laminar flame-thickness $\delta_{fl} \simeq 0.019\, D$.

Spatial discretization is based on central second order finite differences in conservative form on a staggered grid. The convective terms of the relevant reaction-advection-diffusion equations for the scalars are discretized by a bounded central difference scheme designed to avoid spurious oscillations [23]. This non-linear scheme imposes the boundness property characteristic of the convection terms without introducing a large extra-dissipation as in classical TVD schemes. Temporal evolution is performed by a low-storage third order Runge-Kutta scheme [24].

Velocity is prescribed (Dirichlet condition) at the inflow section, by using a cross-sectional plane of a periodic turbulent pipe flow, provided by a companion time-evolving DNS. A convective outflow condition is adopted together with a traction-free condition at the side boundary which mimics the open environment surrounding the flame. The DNS reproduces a premixed Bunsen flame with Reynolds number based on diameter D equal to $Re_D = U_0 D/\nu_\infty = 6000$, with U_0 the bulk velocity, ν_∞ the kinematic viscosity of the cold flow.

The computational domain, $[\theta_{max} \times R_{max} \times Z_{max}] = [2\pi \times 12.34 \times 14]R$, is discretized by $N_\theta \times N_r \times N_z = 128 \times 201 \times 560$ nodes with radial mesh stretching for accurate resolution of the shear layer. The grid size in the jet region is about two/three times the Kolmogorov scale allowing also for an accurate description of the instantaneous flame front. More details on the code can be found in [15, 14] for incompressible jets and in [21] for the reactive case.

Particles evolve by a Lagrangian tracking method which integrates equation (1) by means of the same Runge-Kutta method used for the fluid phase. Interpolation of fluid velocity at particle positions is done by using mixed second/third order Lagrangian polynomials. Particles are assumed to be diluted and do not counteract on the flow (one-way coupling). In this limit the dynamical effect of inter-particle collisions can be safely neglected [2]. Nonetheless it should be remarked that also results obtained in the one-way coupling regime may be useful to model collision kernels, see e.g. [3]

Four particle populations are considered to mimic a laboratory Bunsen premixed flame seeded with alumina particles ($\rho_p = 4000\ kg/m^3$) with diameters $d_p = 1\mu m$, $d_p = 5\mu m$, $d_p = 10\mu m$, $d_p = 20\mu m$. In the four cases the flamelet Stokes number is respectively $St_{fl} = 0.022$, $St_{fl} = 0.54$, $St_{fl} = 2.16$, $St_{fl} = 8.65$, while the inlet Stokes number based on the Kolmogorov time scale is about half the flamelet Stokes number $St_\eta \simeq St_{fl}/2$.

Particles are introduced in the field at a fixed rate with homogeneous distribution at the jet inlet section with velocity matching the local fluid. About six million particles are evolved in the simulation.

The simulation runs for $30\, D/U_0$ to achieve a statistical steady state before collecting about one hundred fields, separated by $0.125\, D/U_0$, for statistical analysis.

The left panel of figure 1 provides a slice of the instantaneous fluid axial velocity field (contours) and of the position of the flame front localized by the reactant iso-level $Y_R/Y_R^0 = 0.5$ (black solid line). The turbulent pipe flow originates a fully turbulent inflow for the Bunsen jet so that the instantaneous flame front appears highly wrinkled. The right panel of figure 1 reports the instantaneous configuration of the smallest particles ($St_{fl} = 0.022$) where the effect of the abrupt expansion across the flame front appears.

4. Particle clustering

The instantaneous configuration of the four particle populations is presented in figure 2. Colors denote the fluid density at particle positions and allow to detect the flame front. The huge variations in the particle concentration across the flame front is induced by the sudden expansion due to heat release. According to their inertia, the particles can differently follow the abrupt acceleration experienced by the fluid. Actually for larger particles, the effect is not restricted just beyond the flame front, but the particle distribution is influenced well into the burned gas region.

The clustering, apparent in figure 2, takes place at smaller and smaller scales as the Stokes number is reduced. The clusters in the burned region are particularly well defined for intermediate weight particles, $St_{fl} = 0.54$ and 2.16, with the typical length scale of the voids large enough to be clearly detected. The lightest particles are more evenly distributed both in the burned and unburned regions recovering a tracer-like behavior characterized by a sharp jump of the particle density across the front.

Particle segregation can be measured by the deviation of the actual particle distribution with respect to randomly distributed independent positions. These reference conditions are expressed by the Poisson distribution giving the probability $p(n)$ to find n particles in a certain domain Ω of volume ΔV with characteristic length $\ell = \sqrt[3]{\Delta V}$. Once the average particle number $\bar{n}$ is known, the probability density function (pdf) reads:

$$P\left(n, \bar{n}\right) = \frac{\bar{n}^n e^{-\bar{n}}}{n!}. \tag{8}$$

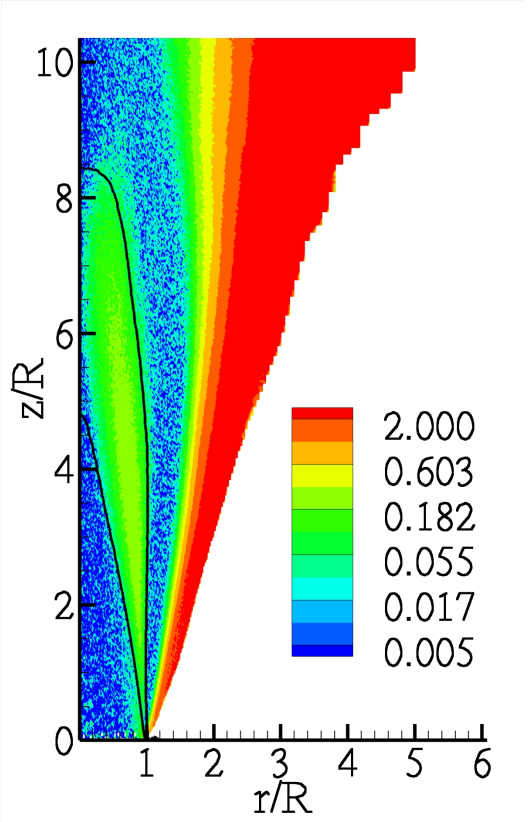

Figure 3. Clustering Index field K (contour) for the smallest particles ($St_{fl} = 0.022$). The control volumes correspond to the computational cells allowing to exploit the azimuthal homogeneity for the statistics, so the typical dimension becomes $\ell \propto r^{1/3}$. The solid lines indicate the boundaries of the flame brush, here identified by the isolevels of the mean progress variable $\bar{c} = 1 - Y_R/Y_R^0 = 0.05$ and $\bar{c} = 1 - Y_R/Y_R^0 = 0.95$.

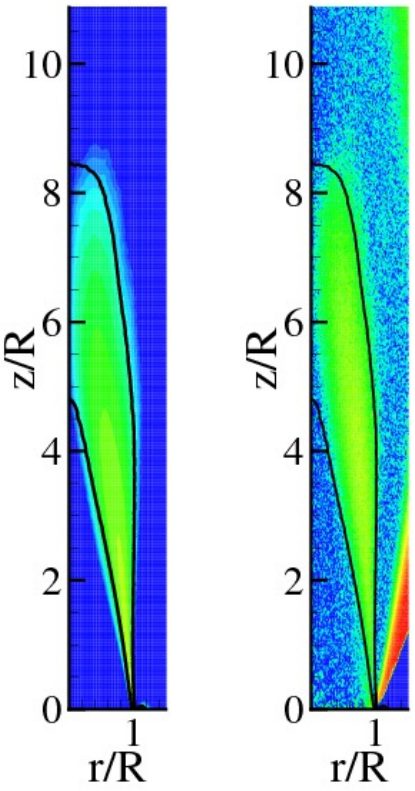

Figure 4. Clustering index K: model (13), left panel, and numerical results, right panel. The control volumes correspond to the computational cells allowing to exploit the azimuthal homogeneity for the statistics, so the typical dimension becomes $\ell \propto r^{1/3}$. The solid lines indicate the boundaries of the flame brush, here identified by the isolevels of the mean progress variable $\bar{c} = 1 - Y_R/Y_R^0 = 0.05$ and $\bar{c} = 1 - Y_R/Y_R^0 = 0.95$.

Since the variance of Poissonian processes $\sigma_n^2 = \overline{(n-\bar{n})^2} = \overline{(\delta n)^2}$ equals the mean value $\bar{n}$ a measure of particle clustering is provided by the clustering index K, see e.g. [17], which is based on the departure from the Poissonian distribution,

$$K = \frac{\overline{(\delta n)^2}}{\bar{n}} - 1. \tag{9}$$

Obviously a Poissonian distribution implies $K = 0$, due to the absence of any clustering or preferential localization effect. A negative clustering index $K < 0$ instead corresponds to a more uniformly distributed particle configuration characterized by a smaller ratio of the variance with respect to the mean value. On the contrary, if particles preferentially aggregate in clusters, the variance exceeds the mean value, yielding a positive clustering index, $K > 0$. Since the clustering index depends on the length scale ℓ, $K(\ell)$, via $\bar{n}(\ell)$ and $\overline{(\delta n)^2}(\ell)$, all the above features are scale dependent. Additionally for inhomogeneous processes the clustering index becomes a field since it depends on the position of the control domain $\Omega(\boldsymbol{x})$, $K = K(\boldsymbol{x}, \ell)$.

The clustering index field can be exploited to quantify the amount of particle segregation induced by the fluctuating turbulent flame front. An example is reported in figure 3 for particles with flamelet Stokes number 0.022 and control volumes corresponding to the computational mesh cells. The region spanned by the flame front is called the flame brush. It can be defined in terms of the average progress variable $\bar{c}$, where the instantaneous progress variable $c = 1 - Y_R/Y_R^0$ ranges from 0 in the reactants to 1 in the products. The flame brush is then the region where $0 < \bar{c} < 1$ whose boundaries are shown as thick lines in figure 3. The clustering index K, shown by colors in the same figure, is positive in the flame brush and in the outer region of the jet. In the outer region the huge value of the clustering index is induced by the intermittency of the boundary between the hot jet seeded with particles and the external, particle-free, cold environment. Such process leads to a particle distribution characterized by a large value of K. More interesting for our purpose is the flame brush region which is spanned by the instantaneous flame front. Away from these two regions, the clustering index almost vanishes suggesting an almost purely Poissonian arrangement of these quasi-Lagrangian particles at $St_{fl} \ll 1$.

As shown in the figure, the clustering observed in the flame brush is remarkable also for very light particles. To try and explain this effect of the flame we resort to the Bray-Moss-Libby (BML) description of the flamelet [18] and to the assumption of a Poissonian distribution for the particles in the two nearby regions, burned and unburned gases respectively. We remark that in order to apply the BML formalism, the control volume where we count the particle number should contain only a single state of the mixture, either burned or unburned gas. These assumptions, which are exact for tracers, are reasonable also for sufficiently small particles ($St_{fl} \ll 1$) whenever the instantaneous flame front is thin.

In the flamelet context the state of the mixture is either $c = 0$ (unburned) or $c = 1$ (burned), and the probability distribution is $p(\boldsymbol{x}, c) = [\alpha(\boldsymbol{x})\delta(c) + \beta(\boldsymbol{x})\delta(1-c)]$, where α and β are the probability to find the unburned or burned gases at $\boldsymbol{x}$. By evaluating $\bar{c}$ from the above pdf it follows $\beta(\boldsymbol{x}) = 1 - \alpha(\boldsymbol{x}) = \bar{c}(\boldsymbol{x})$, see [18, 25]. Let us now address the joint probability distribution of particle number in the volume V and instantaneous progress variable c, $p(\boldsymbol{x}; c, n) = p(\boldsymbol{x}, c)\, p(n|c)$. We shall assume that the conditional probability of the particle number conditioned to the state c of the mixture is Poissonian both for the burned and unburned state. In these conditions the conditional probability is entirely determined by the average particle number conditioned to the state of the mixture, $\langle n|c\rangle$, $p(n|c) = P(n; \langle n|c\rangle)$ where P is the Poissonian distribution, eq. 8. It follows

$$p(\boldsymbol{x}; c, n) = \{[1 - \bar{c}(\boldsymbol{x})]\, \delta(c) + \bar{c}(\boldsymbol{x})\delta(1-c)\}\; P(n; \langle n|c\rangle). \tag{10}$$

Starting from 10 we can express the first and second order moments of the particle number pdf,

$$\bar{n}(\boldsymbol{x}) = [1 - \bar{c}(\boldsymbol{x})]\overline{n_u} + \bar{c}(\boldsymbol{x})\overline{n_b} \tag{11}$$

$$\overline{n^2}(\boldsymbol{x}) = [1 - \bar{c}(\boldsymbol{x})]\overline{n_u^2} + \bar{c}(\boldsymbol{x})\overline{n_b^2} \tag{12}$$

where $\bar{n}_{u/b}$ is the mean particle number in the volume V corresponding to fully unburned and burned conditions. Under our assumptions these two quantities are strictly related to the density a purely Lagrangian tracer would have in corresponding conditions. It is than clear that, according to our model, the ratio $\bar{n}_u/\bar{n}_b$ equals the gas density ratio across the thin flame front which is estimated by the expansion ratio $\tau = T_b/T_u$, $\bar{n}_u/\bar{n}_b = \tau$. Considering equations (9), (11) and (12), the clustering index reads,

$$K_0(\boldsymbol{x}) = \frac{\overline{n}_u}{\tau} \frac{\bar{c}(\boldsymbol{x})[1 - \bar{c}(\boldsymbol{x})]\,(\tau - 1)^2}{\bar{c}(\boldsymbol{x}) + \tau[1 - \bar{c}(\boldsymbol{x})]}. \tag{13}$$

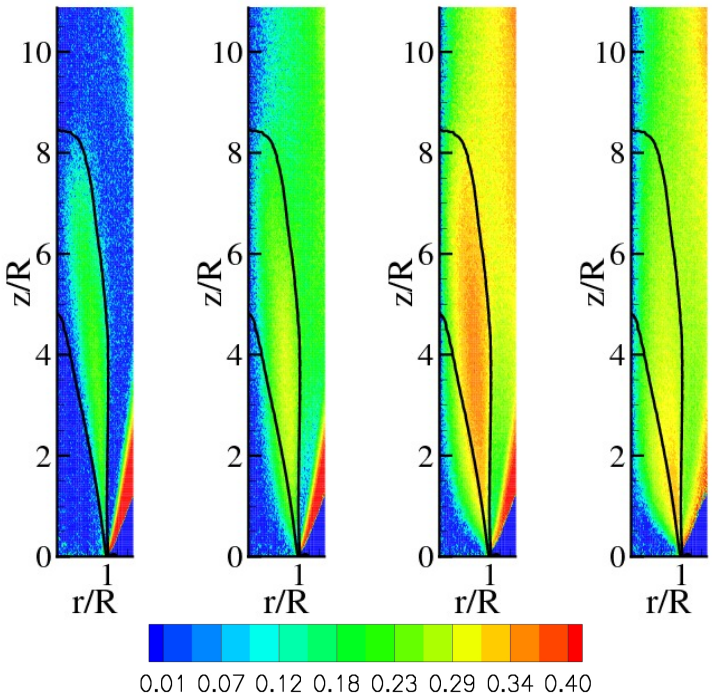

Figure 5. Contours of the Cluster Index for all particle populations; from left: $St_{fl} = 0.022$, $St_{fl} = 0.54$, $St_{fl} = 2.16$ and $St_{fl} = 8.65$, respectively. The control volumes correspond to the computational mesh cells. The lines indicate two isolevels of the mean progress variable $\bar{c} = 1 - Y_R/Y_R^0 = 0.05$ and $\bar{c} = 1 - Y_R/Y_R^0 = 0.95$.

Hence the clustering index deviates from zero only in the flame brush where $0 < \bar{c} < 1$, to vanish in the burned and unburned region where the statistics comes back to Poissonian.

Relation (13) highlights that for light particles, a positive clustering index, $K_0 > 0$, is mainly due to the fluctuation of the thin flame front. A Poissonian distribution is obviously recovered in the limit of $\tau \to 1$. The model proposed for the flame brush region can be easily extended to model the behavior of the particles in the intermittent region separating the burned gas and the external particle-free environment. To this purpose we shall assume that the instantaneous interface between hot gas and environment is sufficiently thin, as expected for high Reynolds number flows. Across the instantaneous interface the average particle number jumps from $\bar{n}_b$ to $\bar{n}_e = 0$. Denoting by $\tau_e = \bar{n}_b/\bar{n}_e \to \infty$, the empty external region is formally characterized by a limiting Poissonian process with vanishing average particle number. According to the model the clustering index pertaining to this outer part of the jet is described by relation (13) in the limit $\tau \to \infty$ with $\bar{n}_u$ replaced by $\bar{n}_b$, i.e. $K_0 = \bar{n_b}\bar{c}_e(\boldsymbol{x})$. In full analogy with the flame brush, the instantaneous indicator function $c_e(\boldsymbol{x})$ has a singular bi-modal distribution taking the value 0 in the fully burned region and 1 in the external fluid while its average $\bar{c}_e$ goes smoothly from zero to one. The huge value of K, seen in figure 3, in the outer part of the jet can actually be interpreted in this framework, after noting that the relevant Stokes number should be interpreted in terms of the local turbulent time scale which is typically larger than the flamelet characteristic time.

Focusing on the flame brush region, we show in figure 4 the capability of the model to excellently reproduce the numerical results by comparing the DNS data for the smallest particles ($St_{fl} = 0.022$) with the model (13). The vanishing of the clustering index on the axis both in the model and in the DNS is explained by taking in consideration the radial variation of the

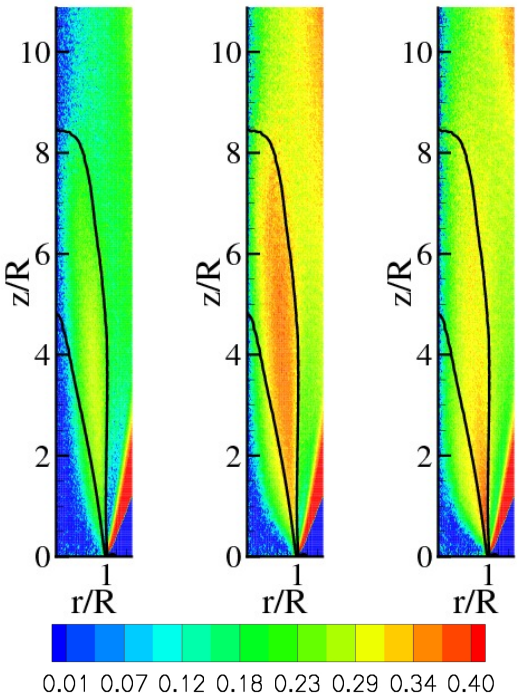

Figure 6. Estimation of the clustering index K using the right hand side of equation (15). From left to right: data concerning particles with $St_{fl} = 0.54$, $St_{fl} = 2.16$ and $St_{fl} = 8.65$, respectively.

coarsening length, which following the grid size is proportional to the cubic root of the radial coordinate, $\ell \propto r^{1/3}$. Consistently the average particle number $\bar{n}_u$ drops to zero towards the axis entailing the vanishing of the clustering index.

Relation (13) and figure 4 show that the quasi-Lagrangian particles, whose inertia is negligible, present a positive clustering index in the flame brush region. This phenomenon suggests that a positive clustering index is induced not only by the interaction between particle inertia and flame front fluctuations or turbulence, but also by the mere dynamics of the flame front that induces a strong decrease in the particle concentration due to the fluid thermal expansion. This peculiar behavior promotes a substantial instantaneous fluctuation of the particle concentration with respect to the local average, which is detected by the clustering index.

The influence of the finite inertia on flame-induced particle clustering is addressed in figure 5 where the clustering index is reported for each particle population. Two features are immediately apparent, the increase of the clustering intensity with increasing inertia and the extension of the clustering region towards the burned gas well outside the flame brush. For the range of parameters we have investigated, the maximum deviation always occurs in the flame brush and we find an overall maximum clustering intensity for particles with $St_{fl} = 2.16$. The observation that peak clustering occurs at flamelet Stokes numbers order one confirms that this is actually the parameter controlling particle localization effects in turbulent premixed flames.

Since inertia increases the clustering index over the already positive value it has for tracers one needs to carefully separate the two effects. To this purpose it is convenient to define the

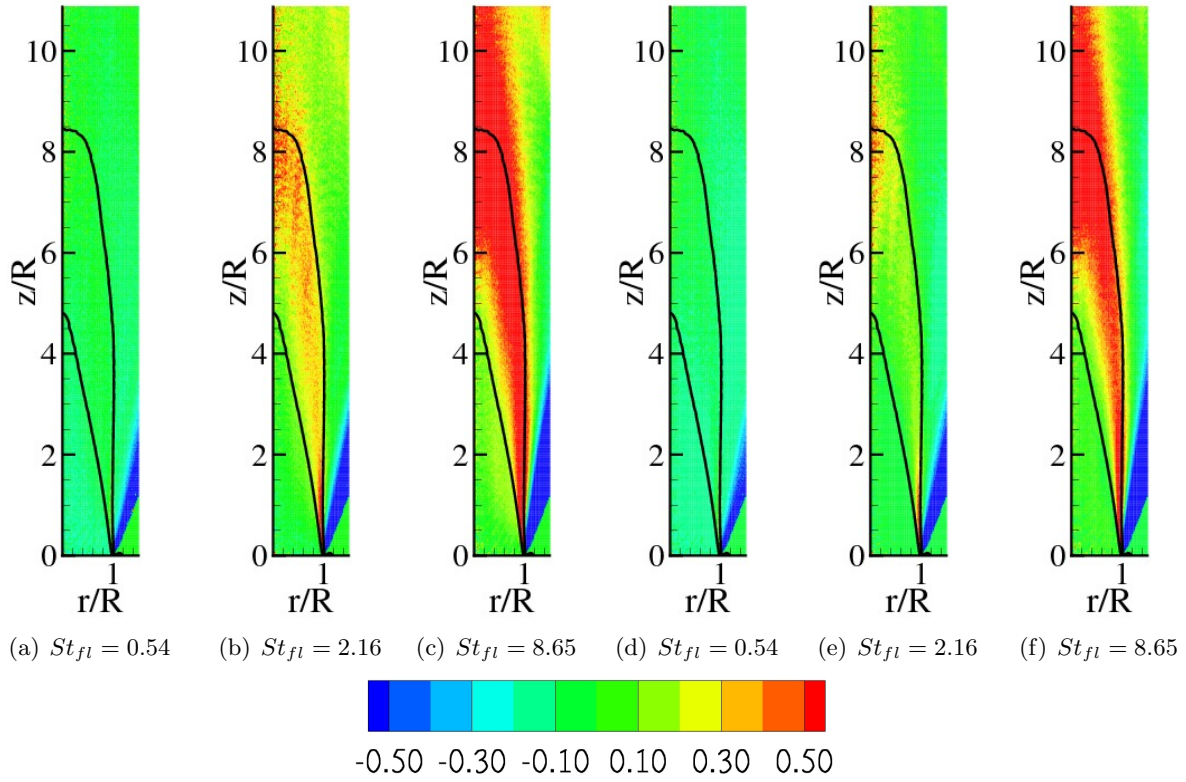

(a) $St_{fl} = 0.54$ (b) $St_{fl} = 2.16$ (c) $St_{fl} = 8.65$ (d) $St_{fl} = 0.54$ (e) $St_{fl} = 2.16$ (f) $St_{fl} = 8.65$

Figure 7. Panels (a)-(b)-(c) represent $\Delta\overline{\delta n^2}/\bar{n}_0$; panels (d)-(e)-(f) represent $(K_0+1)\Delta\bar{n}/\bar{n}_0$. See equation (15) and the related explanation for more details.

mean particle number and its variance as,

$$\bar{n} = \bar{n}_0 + \Delta\bar{n}$$
$$\overline{\delta n^2} = \overline{\delta n_0^2} + \Delta\overline{\delta n^2} \tag{14}$$

where the subscript 0 is referred to tracer-like particles ($St \to 0$) and the two additional terms on right-hand-side quantify the correction due to departure from the reference state of tracers. Inserting relations (14) in definition (9), to first order in the corrections the Clustering index $K(\ell)$ reads,

$$K(\ell) \simeq K_0 + \frac{\Delta\overline{\delta n^2}}{\bar{n}_0} - (K_0+1)\frac{\Delta\bar{n}}{\bar{n}_0} \tag{15}$$

where $K_0 = \overline{\delta n_0^2}/\bar{n}_0 - 1$ is the Clustering index for tracers, eq. (13). In these approximations the effect of inertia are condenced to the last two terms in right-hand-side of equation (15). The first term, $\Delta\overline{\delta n^2}/\bar{n}_0$, takes care of the inertia-induced fluctuation of the particle number in the control volumes. The second term, $-(K_0+1)\Delta\bar{n}/\bar{n}_0$, accounts for the variation of the mean particle number. In fact inertia prevents the particles from quickly responding to the gas expansion implying that their mean number in a fixed volume exceeds that of tracers.
The right-hand-side of equation (15) is represented in figure 6. The excellent agreement between the approximate clustering index estimated by equation (15) and the exact one reported in figure 5 4demonstrates the reliability of the approximations. Figure 7 reports $\Delta\overline{\delta n^2}/\bar{n}_0$ and

$(K_0+1)\Delta\bar{n}/\bar{n}_0$ for particles with $St_{fl} = 0.54; 2.16; 8.65$. Concerning the most segregating particles, $St_{fl} = 2.16$, we observe that $\Delta\overline{\delta n^2}/\bar{n}_0$ is large in the flame brush region, especially near the burned gas side. We infer that the interaction between the corrugated flame front and the particle inertia is a source of particle clustering via an increase of the particle number fluctuation. Since, though small, $(K_0+1)\Delta\bar{n}/\bar{n}_0$ is positive it tends to mitigate the clustering. For this kind of particles ($St_{fl} = 2.16$), $\Delta\overline{\delta n^2}/\bar{n}_0$ is larger than $(K_0+1)\Delta\bar{n}/\bar{n}_0$, resulting in a quite large clustering in the flame brush. For particles with larger inertia, $St_{fl} = 8.65$, both terms increase. In particular $(K_0+1)\Delta\bar{n}/\bar{n}_0$ becomes comparable with $\Delta\overline{\delta n^2}/\bar{n}_0$ resulting in a less intense clustering than before. It is clear that a maximum clustering level should be achieved at intermediate Stokes numbers. The appropriate selection of the physically relevant time scale, the flamelet time scale, normalizes the Stokes number to be order one.

5. Final Remarks

Several issues concerning the behavior of inertial particles in a turbulent reacting jet has been discussed. We found that the flamelet Stokes number which compares particle relaxation time and flame front characteristic time, controls the particle dynamics, see also [21].

Inertial particles aggregate in clusters which are especially evident in the hot gas region. The clustering index was exploited to quantify the amount of clustering as a function of particle inertia.

Since the gas expands the concentration of Lagrangian tracers changes abruptly across the front, in these conditions the front oscillations produce local fluctuations in the tracer concentration which result in a positive clustering index in the flame brush region. This effect is well described by a model based on the Bray-Moss-Libby formalism for flamelets (negligible thickness of the flame front).

Inertia leads to the increase of clustering with respect to this base level. The increase is due to two contributions operating in opposite directions. One is due to the increment of the particle number fluctuation induced by the interaction between fluctuating wrinkled flame front and the particle inertia. This contribution increases with inertia. The other is associated with the increment of the mean particle concentration in the flame brush. Actually inertial particles respond slowly to the expansion of the flow, resulting in a more gentle reduction of the mean particle concentration across the front. This term operates to reduce the clustering.

The competition between the two effects gives rise to a maximum clustering intensity for particle with $St_{fl} = 2.16$. For larger inertia the two effects become comparable resulting in a less intense clustering. The fact that maximum clustering is achieved for $St_{fl} = \mathcal{O}(1)$ confirms that the flow time scale controlling the particle segregation in the flame is the flamelet time scale $\tau_{fl} = \delta_{fl}/\Delta u_{fl}$, where δ_{fl} is the flame thickness and Δu_{fl} is the jump velocity across the instantaneous flame front.

6. Acknowledgements

We want to thank the COST Action MP0806 Particles in Turbulence for supporting the present work.

7. References

[1] Toschi F and Bodenschatz E 2009 *Annual Review of Fluid Mechanics* **41** 375–404
[2] Balachandar S and Eaton J 2010 *Annual Review of Fluid Mechanics* **42** 111–133 ISSN 0066-4189
[3] Sundaram S and Collins L 1997 *Journal of Fluid Mechanics* **335** 75–109 ISSN 0022-1120
[4] Balkovsky R, Falkovich G and Fouxon A 2001 *Physical Review Letters* **86** 2790
[5] Bec J, Biferale L, Cencini M, Lanotte A, Musacchio S and Toschi F 2007 *Physical Review Letters* **98** 084502
[6] Gualtieri P, Picano F and Casciola C 2009 *J. Fluid Mech.* **629** 25
[7] Coleman S and Vassilicos J 2009 *Physics of Fluids* **21** 113301

[8] Reeks M 1983 *J. Aerosol Sci.* **14** 729–739
[9] Rouson D and Eaton J 2001 *J. Fluid Mech.* **428** 149
[10] Marchioli C, Soldati A, Kuerten J, Arcen B, Taniere A, Goldensoph G, Squires K, Cargnelutti M and Portela L 2008 *International Journal of Multiphase Flow* **34** 879–893
[11] Picano F, Sardina G and Casciola C 2009 *Phys. Fluids* **21** 093305
[12] Hardalupas Y, Taylor A and Whitelaw J 1989 *Proceedings of the Royal Society of London. A. Mathematical and Physical Sciences* **426** 31 ISSN 1364-5021
[13] Longmire E and Eaton J 1992 *Journal of Fluid Mechanics* **236** 217–257
[14] Picano F, Sardina G, Gualtieri P and Casciola C 2010 *Physics of Fluids* **22** 051705
[15] Casciola C, Gualtieri P, Picano F, Sardina G and Troiani G 2010 *Physica Scripta* **T142** 014001
[16] Eidelman A, Elperin T, Kleeorin N, Melnik B and Rogachevskii I 2010 *Physical Review E* **81** 56313
[17] Kostinski A and Shaw R 2001 *J. Fluid Mech.* **434** 389–398
[18] Bray K, Libby P A and Moss J 1985 *Combustion and Flame* **61** 87 – 102
[19] Maxey M and Riley J 1983 *Physics of Fluids* **26** 883
[20] Stella A, Guj G, Kompenhans J, Raffel M and Richard H 2001 *Experiments in Fluids* **30** 167–180
[21] Picano F, Battista F, Troiani G and Casciola C 2011 *Experiments in Fluids* **50**(1) 75–88
[22] Majda A and Sethian J 1985 *Combustion Sci. and Tech.* **42** 185
[23] Waterson N and Deconinck H 2007 *J. Computational Physics* **224** 182–207
[24] Lundbladh A, Henningson D and Johansson A 1992 Tech. rep. FFA-TN 1992-28,KTH, Stockholm, Sweden
[25] Troiani G, Marrocco M, Giammartini S and Casciola C 2009 *Comb. and Flame* **156** 608–620